Chemistry Letters

http://www.csj.jp/journals/chem-lett/

Vol.32 No.1
January, 2003

CMLTAG
ISSN 0366-7022

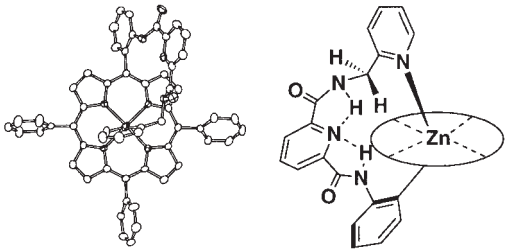

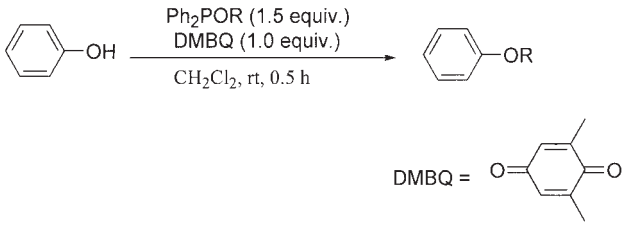

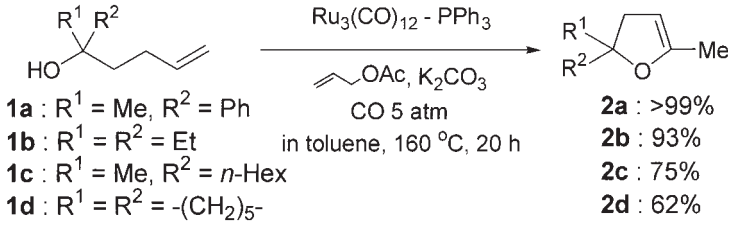

The supported (Ni-Pd) catalysts showed high activity and long life for methane decomposition to form hydrogen and carbon nanofibers of a unique structure.

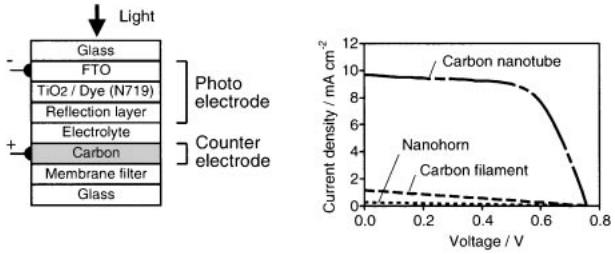

30 **A Novel in situ Template-controlled Route to CuS Nanorods via Transition Metal Liquid Crystals**

Jun Lu, Yan Zhao, Nan Chen, and Yi Xie

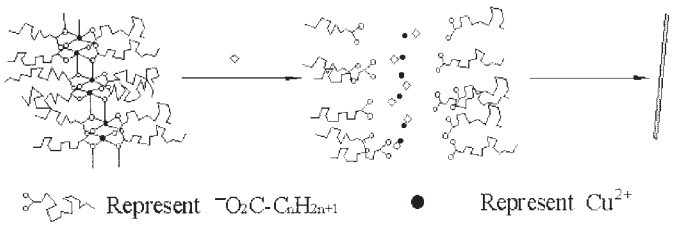

The reaction process of production of CuS nanorods

32 **Electrophosphorescence from Tetrameric Copper (I)-Amide Cluster**

Mitsuharu Noto, Yasuyuki Goto, and Masanao Era

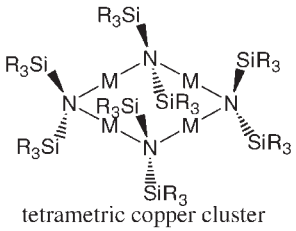

tetrametric copper cluster
M = Cu and R = CH_3

Green electrophosphorescence from a tetrameric copper (I)-amide cluster $[CuN(Si(CH_3)_3)_2]_4$ was successfully observed in the heterostructure device combined with organic carrier transport materials and the copper cluster (peak wavelength = 500 nm, and max. luminance = 400cdm^{-2} at 177 mAcm^{-2} at 22 V).

34 **Gas-Occlusion Properties of a Novel Compound: Mononuclear Copper(II) Terephthalate-Pyridine**

Tetsushi Ohmura, Wasuke Mori, Mari Hasegawa, Tohru Takei, and Akira Yoshizawa

A porous structure, which is formed by hydrogen bonding and self-assembly of the linear copper(II) terephthalate-pyridine, was determined by X-ray crystallography.

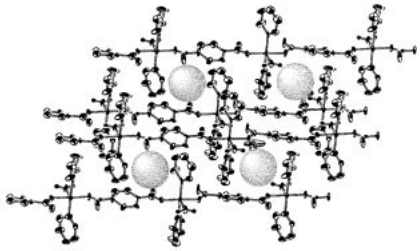

36 **Preparation of Polymer Microspheres in TEOS under Static Condition**

Dongjun Wang, Chenbin Gu, Yongguo Zhou, Xinqiu Wang, Zhen Zhen, Fangqiong Tang, and Xinhou Liu

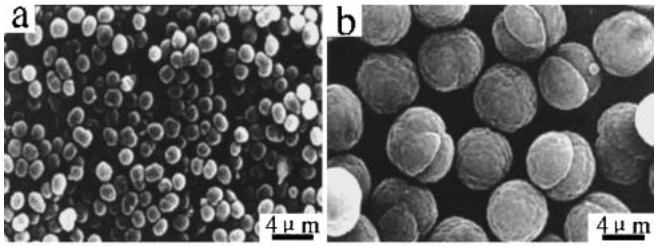

38 **A Novel Route towards Iron- and Chromium-containing MCM-41 Materials through Melt-exchange of the Template**

Athanasios B. Bourlinos, Michael A. Karakassides, Dimitrios Gournis, Vasilios Georgakilas, and Aliki Moukarika

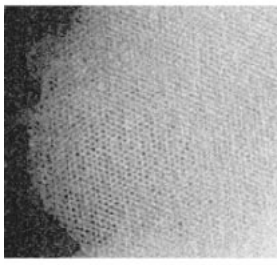

40 **A New Conjugated Polymer Chemosensor Functionalised with 2,6-Bis(1,3,4-oxadiazole-2-yl)pyridine for Metal Ion Recognition**

Nam Choul Yang, Jae Kyun Jeong, and Dong Hack Suh

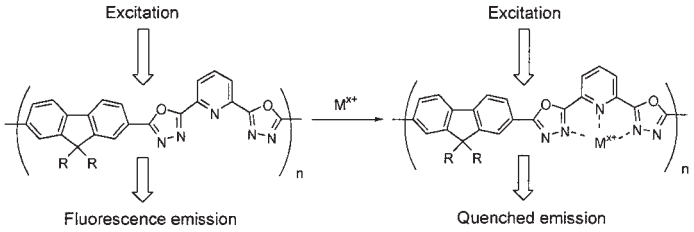

42 **Effect of Calcium on the Catalysis of Nickel in the Production of Crystallized Carbon from Lignocresol for Electromagnetic Shielding**

Xiao-Shui Wang, Noriyasu Okazaki, Tsutomu Suzuki, and Masamitsu Funaoka

LC (lignocresol) added with nickel and calcium produced chars with turbostratic structure carbon (T-component) that could afford a practical electromagnetic shielding capacity at 50-800 MHz, although the addition of nickel alone gave amorphous carbon.

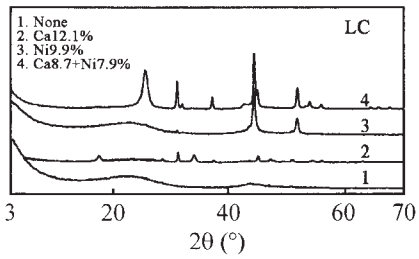

44 **A New Chiral Host, (5*S*-*trans*)-11b-(1,1-Dimethylethyl)-2,3,5,6,11,11b-hexahydro-3-oxo-1*H*-indolizino[8,7-*b*]indole-5-carboxylic Acid Methyl Ester: Complexation by a Helical Network**

Hajime Irikawa, Masanori Morinaga, and Mitsuru Kondo

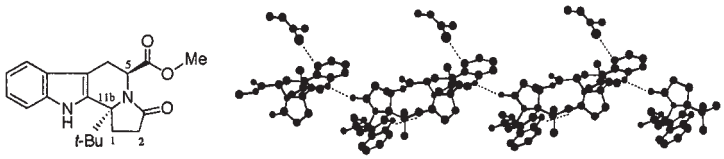

46 **A Short Synthesis of Dipalmitoylphosphatidylinositol 4,5-Bisphosphate via 3-*O*-Selective Phosphorylation of a 3,4-Free Inositol Derivative**

Fushe Han, Minoru Hayashi, and Yutaka Watanabe

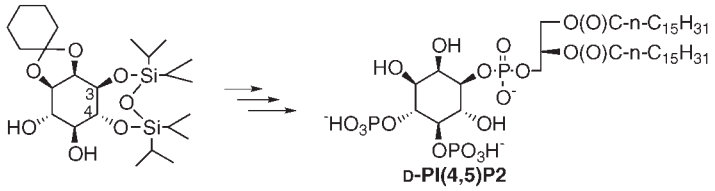

The D-PI(4,5)P2 synthesis involves 3-*O*-selective phosphorylation using the phosphite-pyridinium tribromide method and simultaneous removal of the ketal function under hydrogenolysis in an aprotic solvent, AcOEt.

48 **Topotactic Preparation of Preferentially Oriented $BaTiO_3$ and TiO_2 Thin Films on Polycrystalline Substrate**

Qi Feng, Koji Kajiyoshi, and Kazumichi Yanagisawa

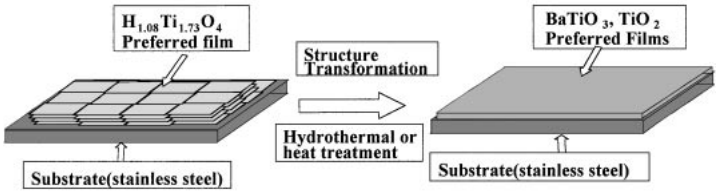

50 **Low-temperature Complete Combustion of Methane over CeO_2-Promoted Pd/HZSM-5 Catalyst with Enhanced Activity and Stability**

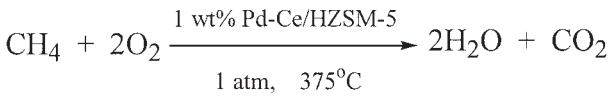

CH_4 Conversion = 100%;
Feed composition: CH_4 (2%), O_2 (8%) and N_2 (90%);
Gas Hourly Space Velocity = 48000 h^{-1}.

Chun-Kai Shi, Le-Fu Yang, and Jun-Xiu Cai

52 **Novel Utilization of Impedance Measurement for Electrochemical Biosensing Aiming at Elimination of Influence by Interference Materials**

Electrochemical oxidation of glucose using the glucose oxidase and an electron mediator gives semicircle Nyquist plots, from which glucose concentration can be determined without influence by interference materials.

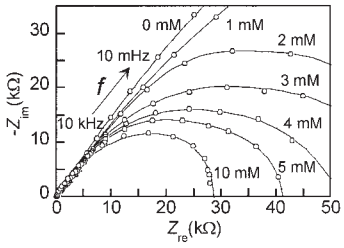

Susumu Kuwabata, Hidefumi Hasegawa, and Kenji Kano

54 **Bilirubin Oxidase and $[Fe(CN)_6]^{3-/4-}$ Modified Electrode Allowing Diffusion-controlled Reduction of O_2 to Water at pH 7.0**

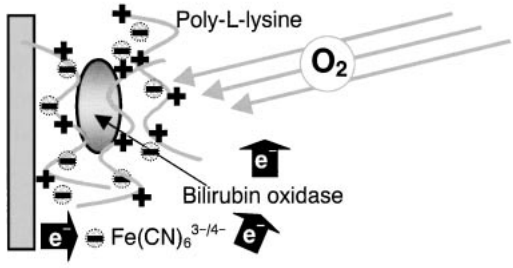

Takaaki Nakagawa, Seiya Tsujimura, Kenji Kano, and Tokuji Ikeda

56 **Lewis Base Catalyzed Michael Reaction between Ketene Silyl Acetals and α,β-Unsaturated Carbonyl Compounds**

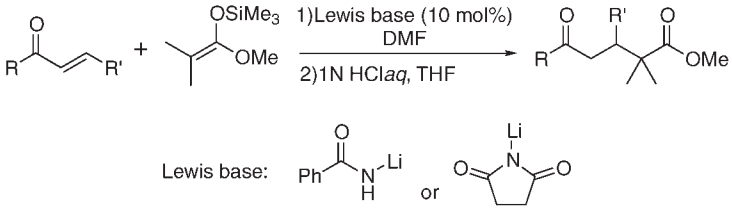

Teruaki Mukaiyama, Takashi Nakagawa, and Hidehiko Fujisawa

58 **Clean Synthesis of 3,3′,5,5′-Tetra-*tert*-butyl-4,4′-diphenoquinone from the Oxidative Coupling of 2,6-Di-*tert*-butylphenol Catalyzed by Alkali-promoted Cu–Mg–Al Hydrotalcites in the Presence of Molecular Oxygen**

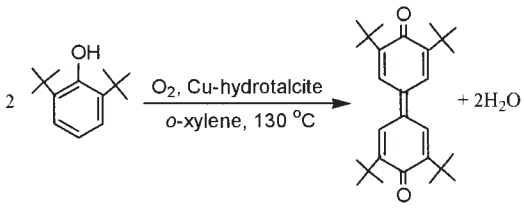

Keisuke Iwai, Takayoshi Yamauchi, Keiji Hashimoto, Tomoo Mizugaki, Kohki Ebitani, and Kiyotomi Kaneda

60 **Structural Change of $Li_{1-x}Ni_{0.5}Mn_{0.5}O_2$ Cathode Materials for Lithium-ion Batteries by Synchrotron Radiation**

Yoshinori Arachi, Hironori Kobayashi, Shuichi Emura, Yoshiyuki Nakata, Minoru Tanaka, and Takeshi Asai

The structural change and charging process for a layered $Li_{1-x}Ni_{0.5}Mn_{0.5}O_2$ were determined by X-ray diffraction and XAFS measurement.

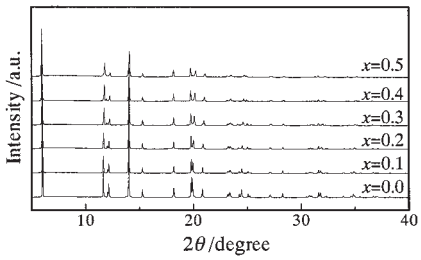

62 **Photoexcited Crystallography of Diplatinum Complex by Multiple-exposure IP Method**

Yoshiki Ozawa, Madoka Terashima, Minoru Mitsumi, Koshiro Toriumi, Nobuhiro Yasuda, Hidehiro Uekusa, and Yuji Ohashi

The Pt–Pt bond shrinkage of the $[Pt_2(pop)_4]^{4-}$ complex has been directly observed by X-ray crystal structure analysis using synchrotron radiation.

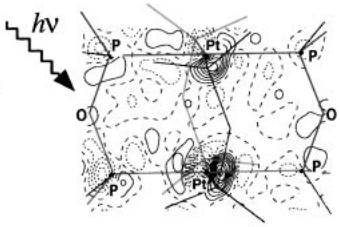

64 **Electronic Structure of $InTaO_4$ with Monoclinic Structure**

Shigenori Matsushima, Hiroyuki Nakamura, Masao Arai, and Kenkichiro Kobayashi

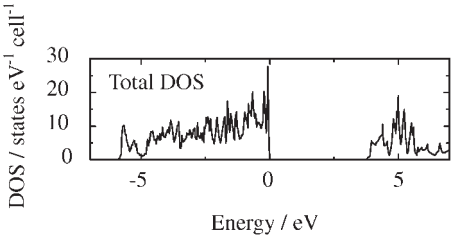

66 **Intramolecular C–H and C–O Bond Activation of Dimethylplatinum(II) Complexes Having the PN Ligand**

Yasutaka Kataoka, Tatsuya Nakamura, and Kazuhide Tani

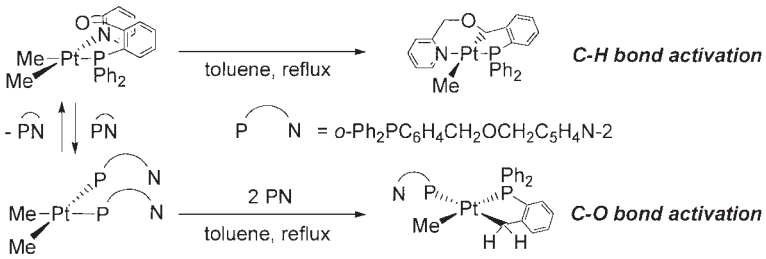

68 **Electron Transport across Vesicle Bilayers Sensitized by Pyrenes: Design and Syntheses of Unsymmetrically Substituted Bifunctional Pyrenes Acting as Excellent Sensitizers**

Asako Yoshida, Akitomo Harada, Tadashi Mizushima, and Shigeru Murata

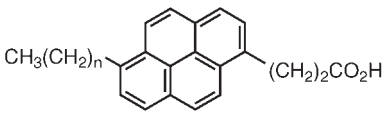

5a; n = 7, **5b**; n = 11

Excellent sensitizers for electron transport across vesicle bilayers

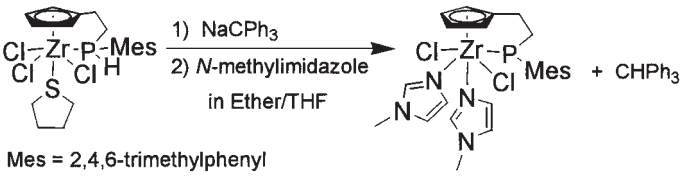

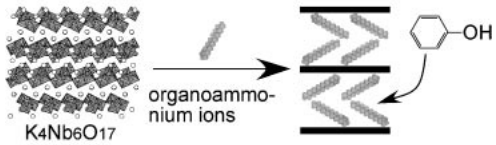

Giant magnetoresistance material $La_{0.5}Sr_{0.5}MnO_3$ has been synthesized under mild hydrothermal condition of 240°C. The morphology of the $La_{0.5}Sr_{0.5}MnO_3$ is cubic single crystal, and the size up to 5 μ m.

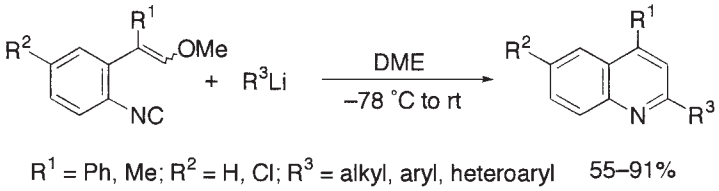

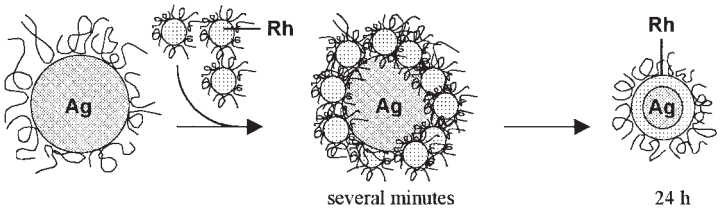

Physical mixture of polymer-protected Ag and Rh nanoparticles spontaneously generates the bimetallic nanoparticles with Ag-core/Rh-shell structure.

80 **Direct Observation of the DNA Multimolecule Condensation with Fluorescence Microscopy**

Lian-Sheng Ling, Xiao-Hong Fang, Chen Wang, Li-Jun Wan, Chun-Li Bai, and Dong-Min Chen

λ-DNA formed 40μm Rod-Like superhelical structure with diameter of 7μm in the presence of 20mmol • l^{-1} spermine. Such big compacted DNA structure is firstly observed. This result is a good complementary to DNA condensation structure reported by other methods.

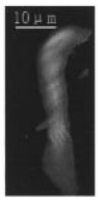

DNA condensation

82 **Efficient Ring Opening Reactions of *N*-Tosyl Aziridines with Amines and Water in Presence of Catalytic Amount of Cerium(IV) Ammonium Nitrate**

Tushar K. Chakraborty, Animesh Ghosh, and T. Venugopal Raju

While *N*-tosyl aziridines were opened very efficiently with amines giving diamines, openings with water required a catalytic amount of cerium(IV) ammonium nitrate.

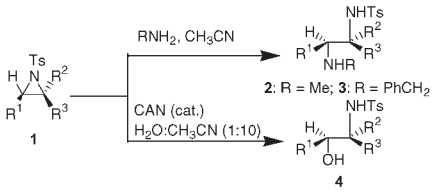

84 **Hydrogen-bonded Macrocluster Formation of Ethylene Glycol on Silica Surfaces in Ethylene Glycol-Cyclohexane Binary Liquids**

Kazue Kurihara, Yasuhiro Nakagawa, and Masashi Mizukami

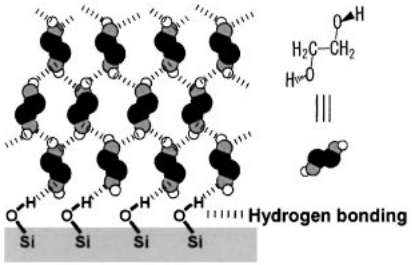

A plausible model of ethylene glycol macroclusters on glass surfaces in cyclohexane.

86 **Development of a Composite Optical Waveguide Sensor for Immunoglobulin G**

Abliz Yimit, Xiuzhu Huang, Yitai Xu, Takashi Amemiya, and Kiminori Itoh

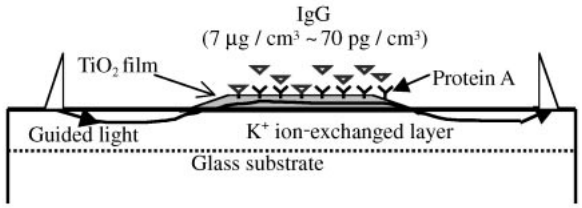

Protein A - TiO_2 film / K^+ ion-exchanged glass COWG immunosensor.

88 **Photo-enhancement of Transfection Efficiency with a Novel Azobenzene-based Cationic Lipid**

Takeshi Nagasaki, Katsutoshi Wada, and Seizo Tamagaki

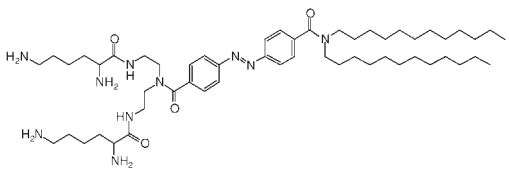

90 **Helical Assembly Formed by Chiral [11]Thiaheterohelicene Molecules in Crystals. Architecture with Triple Helix**

Hiroko Nakagawa, Jun Yoshino, Koh-ichi Yamada, and Motoo Shiro

The crystal structure of a (*P*)[11]thiaheterohelicene demonstrates huge helical assemblies along the *c* axis, in which three crystallographically independent molecules form a smaller right-handed helix.

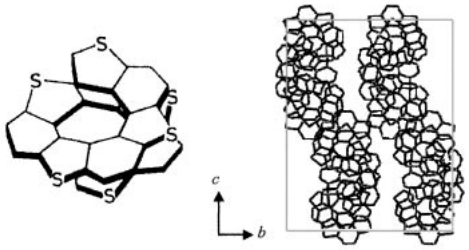

92 **Visible Light-induced Cationic Polymerization of Epoxides Sensitized by Benzoquinonylsulfanyl Derivatives**

Kanji Suyama, Weihong Qu, Masamitsu Shirai, and Masahiro Tsunooka

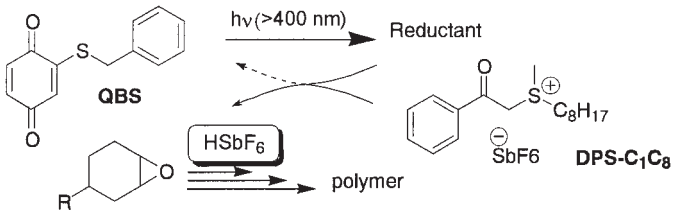

94 **Synthesis of Mesoporous Silicon Oxynitrides via Direct Nitridation with Nitrogen**

Mahendra P. Kapoor and Shinji Inagaki

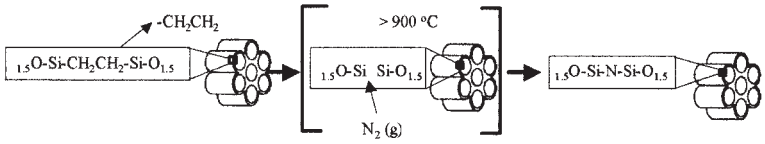

96 **Extraction of Cd(II) and Zn(II) with Dialkylthiophosphinic Acid and Hexadentate Nitrogen-donor Ligand**

Kenji Takeshita, Kunio Watanabe, Yoshio Nakano, and Masayuki Watanabe

The extraction percent of Cd is little changed and that of Zn is decreased remarkably by adding TPEN. TPEN acts as a strong masking agent only for Zn.

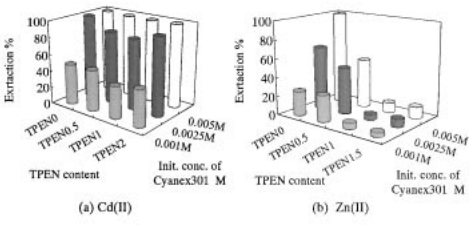

98 **$Ru(bpy)_3^{3+}$ Electrochemiluminescence Detection of Aliphatic and Aromatic Amines with Diketene**

Kazuo Uchikura

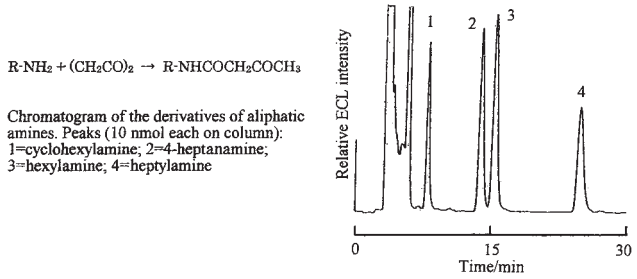

100 **Synthesis of SnO_2 Nanoribbons by Direct Oxidation of Tin Powders**

Xianghua Kong, Dapeng Yu, and Yadong Li

A new method has been successfully developed to synthesize SnO_2 nanoribbons in a large scale by direct oxidation of tin powders.

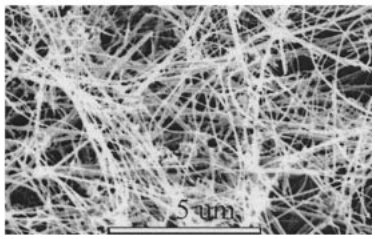

102 **Solid Surface Enhancement Effects on Chemiluminescence: Influence of Cationic Species in Solid Media**

Tetsutaro Yoshinaga, Shigekazu Akimoto, Shinichi Takemura, Hiroshi Hiratsuka, Miki Hasegawa, Michio Kobayashi, and Toshihiko Hoshi

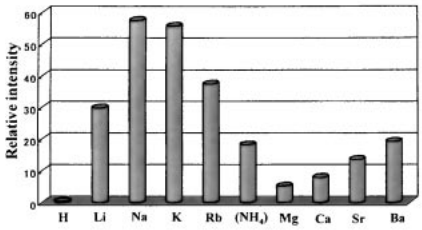

Influence of cationic species on solid surface chemiluminescence has been shown. Alkaline metal ions in salicylates as media solids have shown an interesting tendency with sodium salt as the highest enhancer

104 **Double Elimination Protocol for Access to Unsymmetrical Di(phenylethynyl)benzenes**

Akihiro Orita, Fangguo Ye, Atsushi Doumoto, and Junzo Otera

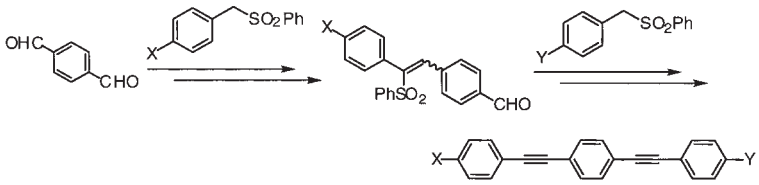

106 **Unique Three-dimensionally Expanded Nanoporous Structure Constructed with a Cu(I) and *cis,cis*-1,3,5-Triaminocyclohexane Having a 3-Fold Axial Symmetry**

Hidekazu Arii, Yamato Saito, Yasuhiro Funahashi, Koichiro Jitsukawa, and Hideki Masuda

The coordination polymer with nanopore was synthesized using $[Cu^{I}(MeCN)_4]SbF_6$ and *cis*,*cis*-1,3,5-triaminocyclohexane.

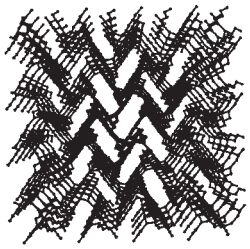

108 **Thermostable Synthetic Hemoproteins: Thermophilic Xylanases Hybridized with Dioxygen-Carrying *meso*-Tetrakis(*o*-pivalamidophenyl)porphinatoiron(II) Derivative**

Teruyuki Komatsu, Seiji Ishihara, Eishun Tsuchida, Hiroyuki Nishide, Chihiro Morokuma, and Satoshi Nakamura